



Advancing identification of drivers of groundwater head change using commonly available observed hydroclimate data

Meeta Gupta^{1,2,3}, Tim Peterson²

¹IIT Bombay-Monash Research Academy, Mumbai, Maharashtra, India

5 ²Department of Civil and Environmental Engineering, Monash University, Clayton, Victoria, Australia

³Centre for Technology Alternatives for Rural Areas, Indian Institute of Technology (IIT) Bombay, Mumbai, Maharashtra, India

Corresponding author: Meeta Gupta (meeta.gupta@monash.edu; meetagupta91@gmail.com)

Abstract. Groundwater depletion in arid and semi-arid regions is a pressing global challenge, driven by intensive extraction for irrigation and compounded by climate variability. However, distinguishing between the impacts of anthropogenic pumping and climate variability on groundwater dynamics remains difficult due to the lagged response of groundwater levels and the scarcity of long-term abstraction records. This uncertainty limits effective groundwater management. Previous studies classify climate-dominated sites using time-series models based primarily on calibration fit rather than predictive performance. Here, we advance groundwater driver attribution by explicitly predicting groundwater heads 2 to 8 years ahead in addition to calibration fit, using commonly available climate data and observed groundwater heads. We undertake this by assessing calibration and predictive performance across 92 wells in North Gujarat, western India, using the HydroSight time-series model. By integrating probabilistic forecasting metrics, particularly the Continuous Ranked Probability Score (CRPS), with traditional calibration measures - Coefficient of Efficiency (CoE), we identified climate-dominated wells with greater spatio-temporal consistency. CRPS effectively differentiated groundwater wells influenced by climate from those affected by pumping, revealing distinct regional patterns in groundwater dynamics. We identified 37-51% of wells as climate-dominated across multiple prediction periods, primarily in eastern districts, validated by field observations and regional assessments. This study advances groundwater assessment methods by demonstrating limitations of conventional calibration-based approaches and advocating predictive skill evaluation. Our data-driven classification relies on observed groundwater head data to assess climate influence at finer resolution, offering insights at a scale not previously explored. These findings support improved groundwater management strategies and guide sustainable use policies in data-scarce regions.

10
15
20
25



30 1 Introduction

Over the past five decades, groundwater has become the primary water source for agriculture in many water-limited regions worldwide, particularly in arid and semi-arid areas where surface water is scarce or unreliable (Siebert et al., 2010; Morsy et al., 2018; Hoogesteger 2022; McDermid et al., 2023). Its intensive extraction, driven by growing irrigation demands and compounded by climate variability, has led to significant declines in groundwater levels, raising concerns about long-term sustainability (Scanlon et al., 2012; Gorelick & Zhang, 2015; de Graaf et al., 2017). However, attributing changes in groundwater levels to pumping, climate and/or land cover change remains a significant challenge and one that impedes appropriate management actions. This challenge arises because groundwater levels are influenced not only by recent withdrawals but also by past withdrawals and antecedent climate conditions, such as multi-year rainfall deficits or surpluses. Moreover, systematic records of groundwater abstraction are rarely available over the full period of groundwater development, as pumping in many regions started decades before formal monitoring or regulation, with comprehensive metering largely limited to recent decades and a small number of high-income settings. This limited data availability severely constrains efforts to separate the effects of pumping from climate variability, making it difficult to determine whether a decline is caused by overexploitation or climate conditions and, hence, the interventions required.

Several studies have attempted to address this issue by identifying sites where groundwater dynamics are influenced by individual drivers and very often relying on statistical models. In contrast, numerical modeling studies are less frequently used due to their high data requirements for long-term ground observation data for key hydro-meteorological parameters, such as groundwater well installation details, aquifer properties, pumping volumes, and climate records (Famiglietti and Rodell, 2013; Taylor et al., 2013; Condon et al., 2021). Additionally, challenges related to the limited understanding and modeling of subsurface processes further constrain their applicability (Oreskes et al., 1994; Ojha et al., 2015). Given these challenges, statistical models have been widely used to analyze groundwater dynamics by identifying the influences of climate variability and anthropogenic activities. For example, Shapoori et al. (2015a, 2015b) used the HydroSight time-series model (Peterson and Western, 2014) to decompose groundwater head variations into meteorological and pumping-related components in southeastern Australia. Similarly, Fan et al. (2023) used HydroSight to identify observation bores across Australia dominated by climate rather than pumping. Using deep learning techniques, Wunsch et al. (2022) employed a convolutional neural network (CNN) model to identify sites across Germany where groundwater level trends are primarily driven by climate. While these studies provide valuable insights, the assessment of climate-dominated sites wholly relied on the fit to a calibration period. However, such approaches do not assess the predictive skill. This is crucial because groundwater pumping may vary over time, and models calibrated under specific conditions may fail when those conditions change. More broadly, the ability of a scientific theory or approach to make accurate and verifiable predictions



is a far stronger threshold to meet than one explaining only the dependent data used to establish the theory or approach. Collenteur et al. (2024) recognised the importance of predictive evaluation in their assessment of various groundwater time-series methods, but to date this has not progressed to using predictive evaluation in the attribution of groundwater drivers.

70 However, the prediction of groundwater heads presents challenges because groundwater levels are generally unconstrained by a lower limit (excluding complete dewatering) or an upper limit and exhibit strong serial correlation, leading to pronounced interannual trends in which past conditions often influence future levels for multiple years (Fowler et al., 2020). This leads to a more persistent and lagged response to both climatic and anthropogenic drivers, implying that good agreement between
75 simulated and observed groundwater hydrographs during calibration does not necessarily indicate correct attribution of the underlying drivers. Such difficulties in evaluating groundwater predictions also emerged in Collenteur et al. (2024) whereby multiple performance metrics were required, making the comparison of various approaches across various metrics problematic

In this context, different combinations of climatic and anthropogenic drivers may produce similar
80 groundwater hydrographs when the underlying processes differ. For example, a model may reproduce long-term trends while underrepresenting short-term variability, or capture variability while exhibiting systematic bias in groundwater levels, with both cases appearing consistent with observations when assessed visually or through calibration performance. Consequently, attribution based primarily on hydrograph reproduction remains problematic.

85 Furthermore, it is important to recognize that in many groundwater systems drivers such as groundwater pumping intensity and land use/land cover (LULC) can change over time, leading to shifting system responses not captured during calibration (Scanlon et al., 2012; Tam and Nga, 2018). Previous studies have shown that increased impervious surfaces, vegetation loss, and the conversion of deep-rooted forests to shallow-rooted agricultural land can significantly alter groundwater recharge, with impacts
90 varying by region and land use type (Scanlon et al., 2005; Owuor et al., 2016; Han et al., 2017; Frommen et al., 2021; Siddik et al., 2022). Additionally, shifts in groundwater pumping—driven by irrigation demands, changes in irrigation methods, or seasonal use—can lead to abrupt changes in groundwater levels, further complicating attribution in model calibration (Fabbri et al., 2016; Porhemmat et al., 2018; Frommen et al., 2021; Pool et al., 2022). These non-stationary influences complicate model evaluation
95 and indicate that model assessment should not rely solely on hydrograph fit, but also consider performance under changing conditions. Here, we evaluate groundwater driver attribution by explicitly assessing predictive performance alongside calibration fit. Using the HydroSight time-series modelling framework (Peterson and Western, 2014), we examine groundwater head dynamics based on commonly available climate data, recognizing the limited availability of long-term pumping records. Model
100 performance is then assessed using a range of existing and new performance metrics, including both deterministic and probabilistic measures, to evaluate hydrograph fit during calibration and behavior



under changing conditions. These analyses are applied to 92 groundwater wells across the North Gujarat region in Western India, covering an area of 28,565 km² known for its intensive groundwater pumping.

Below, the study area is first detailed, followed by a description of all the datasets used and their sources
105 in Section 2. Further, the methods to identify the climate-dominated groundwater wells are then outlined
in Section 2, starting with a description of the model, steps for model setup and calibration, selection of
best model configuration, performance metrics, and implementation in the study area. Section 3 details
the results from the model application for climate-dominated groundwater wells in the study area, and
the model's prediction performance. In Section 4, we critically evaluate the adequacy of the model
110 configuration selection and the performance metrics for identifying climate-dominated groundwater
well locations, along with our deliberations for other likely driving factors responsible. Lastly, the
conclusion section summarizes the key findings of the study and the scope of future research.

2 Material and Methods

2.1 Study area

115 North Gujarat, in Western India, is categorized as a semi-arid region as per the Koppen climate
classification (Peel et al., 2007) (Fig. 2). The North Gujarat Region (NGR) covers an area of 28,565
km² and is bounded by the Aravalli range in the north, Kachchh in the western, and Gujarat plains in
the southern and eastern bounds. Administratively, NGR consists of five districts, Aravalli (3,176 km²),
Banaskantha (10,854 km²), Patan (5796 km²), Mahesana (4,458 km²), and Sabarkantha (4279 km²),
120 supporting 15% (89,27,893) of the total population (6,04,39,692) of the Gujarat state (Census of India,
2011).

The NGR receives an average annual precipitation of 450-850 mm with an increasing trend from west
to east. About 95% of annual precipitation is received during the southwest monsoon season (Jun-Sep).
The mean maximum temperature varies from 36° to 42°C (May), and the minimum temperature varies
125 from 9° to 11°C (January).

Geologically, the region is underlain by formations ranging from Pre-Cambrian to recent Quaternary
periods. NGR comprises the Delhi supergroup and Aravalli supergroup of age Paleoproterozoic –
Mesoproterozoic and plutonic rock formations of age Neoproterozoic such as Erinpura granite, Sendraji
Ambaji granite and Makani granite and gneiss rock formations in the north-eastern part of the region.
130 Most of NGR is covered with Quaternary age alluvial and fluvial sediments in the southwestern
direction of the region (GSI, 1970).

NGR is dominated by deep alluvial soils, with loam as the predominant soil texture. The eastern part of
the region consists mainly of clay and sandy clay loam soils, while the western part is characterised
primarily by clay loam with localised areas of silt loam. The majority of the region has gently sloping
135 terrain (0-5%) and is subjected to slight to moderate soil erosion. The soils are moderately well-drained



in most of the region, making them highly favorable for agriculture. Thus, the major land use in the region is agriculture, which covers about 85% of the total area. Over the past two decades, land use and land cover (LULC) changes have been minimal, with groundwater remaining the primary source of irrigation due to the absence of significant surface water resources.

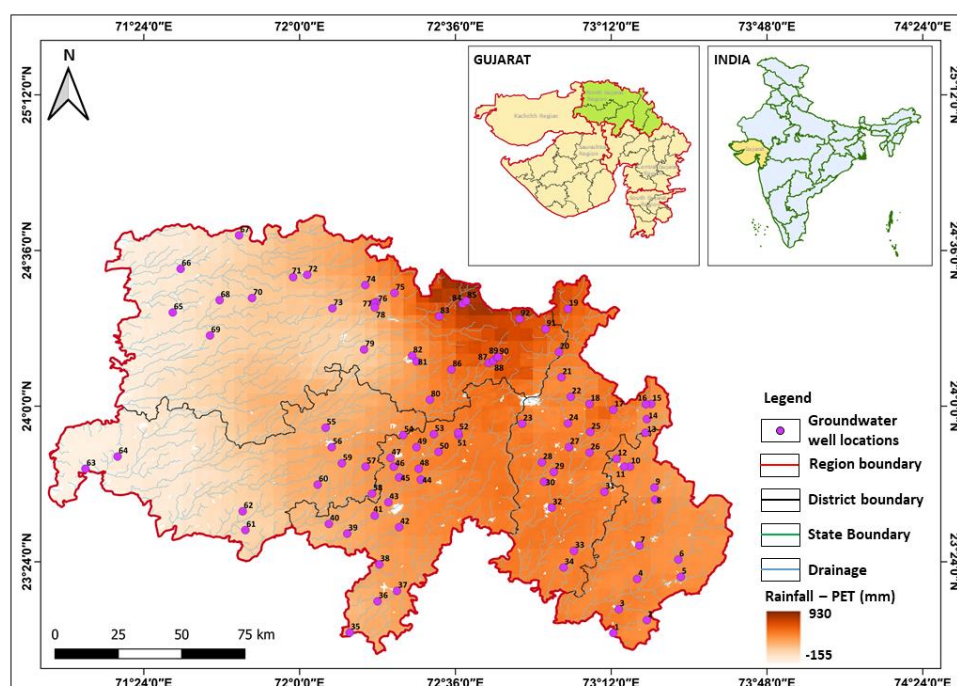
140 NGR aquifer system is grouped into four aquifer groups up to 300 m depth; however, three aquifer groups have been demarcated, i.e., unconfined (up to 90-120 m), semi-confined (up to 180-210 m) and confined (300m) with aquitard (comprising of clay interbedded with thin sand layers) in-between (CGWB, 2020).

The Central Groundwater Board (CGWB), India's groundwater monitoring agency, incorporates the
145 Groundwater Estimation Committee (GEC) 2015 methodology (MoWR, RD & GR, 2017) to estimate groundwater recharge, availability, and extraction using theoretical equations and generalized assumptions. CGWB estimates that NGR has an average annual available groundwater resource equivalent to a depth of 134 mm/year, corresponding to a total volumetric availability of 3.82 billion cubic meters (BCM) that can be extracted for domestic, industrial and irrigation purposes, of which
150 they estimate 95% of the groundwater is extracted. The groundwater is recharged annually through different sources, and the CGWB estimate makes up a total volume of 4.21 BCM, equivalent to an average depth of 147 mm/year across the region (CGWB, 2021). The decadal pre-monsoon assessment in NGR (May 2011-2020) for the monitoring wells installed in the unconfined aquifer suggests that the mean depth to water table range from less than 2 to 40 meters below ground level (m bgl) (CGWB,
155 2022).

However, the rare metering of groundwater usage in the region poses challenges to the accuracy of CGWB's estimates for groundwater extraction and recharge. Groundwater extraction is only approximated over a region using one or a combination of methods, depending on data availability, including the unit draft method, crop water requirement method, power consumption method,
160 consumptive use method, and consumptive use pattern method (MoWR, RD & GR, 2017). Similarly, groundwater recharge is estimated using the water level fluctuation method and the rainfall infiltration factor method (MoWR, RD & GR, 2017). Many of these methods rely on data sourced from existing literature or assumed parameters. The core methods are publicly available, with manuals providing standard equations and procedures. However, the specific steps and assumptions used in practice are
165 not clearly documented, making it challenging to assess their accuracy. Additionally, these estimation approaches suffer from low spatial resolution, reliance on major assumptions, and the confounding effects of climate and pumping add to the uncertainties. Methods such as the unit draft and power consumption approach aggregate data over large administrative units or electricity feeders, ignoring localized hydrogeological variations and individual well efficiencies and make very little use of the
170 historic observed groundwater hydrographs. The crop water requirement and consumptive use methods assume static irrigation efficiency and plant water use, failing to capture variations in farmer behavior



and climatic conditions. Additionally, water table fluctuation-based methods often underestimate recharge, as they attribute all groundwater level declines to pumping, neglecting delayed percolation and soil moisture storage (Healy & Cook, 2002). Errors in rainfall estimates, energy consumption patterns, and assumed parameters can further reduce reliability. Consequently, the estimates for groundwater extraction and recharge are very uncertain and lack consideration of the historic weather data and make little use of the only widely observed groundwater data, which we argue likely lead to an overemphasis on groundwater extraction as the primary driver of depletion.



180 **Figure 1: Location map of North Gujarat region along with select groundwater well locations.**
Spatial variability for the average annual Rainfall -Potential Evapotranspiration (in mm)
estimates (2002-2020) are also mapped.

2.2 Data

2.2.1. Groundwater head data

185 The groundwater time series depth and location coordinates are collected at 493 wells within the region by the CGWB. The groundwater depth is monitored quarterly, i.e., May (pre-monsoon), August (peak monsoon), November (post-monsoon), and January (recession stage) for the unconfined aquifers. These observation wells have been constructed at different times, and for some wells, the monitoring has been stopped after some years. Of the total, 10% of the wells (n = 50) have long-term observations for
 190 groundwater depths for 25 years starting from 1996 till 2020.



For groundwater time series modelling, the length and quality of observations are critical factors that can impact the accuracy and reliability of predictions. Van der Spek and Bakker (2017) showed that the length of the time series is more influential on the groundwater time series model's prediction uncertainty than the total number of observations/observation frequency. Their investigation showed that the shorter length of time series of ≤ 5 years resulted in large predictive uncertainty, while it improved significantly when the time length was increased to 10 years. However, improvements in the model predictive uncertainty were minor in increasing the time lengths to 20 and 30 years. Based on these findings, we required at least 10 years of quarterly groundwater level observations at each groundwater well. Further, we adopted an error model as per the approach of Peterson et al. (2018) that uses the heuristics and double exponential smoothing methods to check the quality of the groundwater level data for any irregular /unreliable observation (as it is very common with groundwater observations) and the serial correlation of the errors. Following the criterion, a total of 92 wells were selected for use (Fig. 2). Detailed information on the data record of all the groundwater wells is shown in Fig. S1. The groundwater depth data of these 92 wells was then transformed into groundwater head using SRTM digital elevation data available at 30 meters spatial resolution. While the SRTM data provides elevations at a relatively coarse spatial resolution, the accuracy of elevations does not influence our results. Further, we conducted a field visit to gain firsthand insights into the history and purpose of these wells, as well as the surrounding influences, to understand the key drivers affecting the groundwater heads.

2.2.2. Climate data

The HydroSight statistical modeling requires daily precipitation and potential evapotranspiration data. Given the lack of meteorological stations in NGR, here we used the Indian Meteorological Department (IMD) gridded meteorological datasets. The precipitation data is available at $0.25^\circ \times 0.25^\circ$ resolution, and the temperature is available at $1.0^\circ \times 1.0^\circ$ resolution. Both products are derived from station observations and provide spatially complete and temporally consistent meteorological inputs. The IMD rainfall dataset has been widely used in hydro-climatological studies across India (e.g., Vinnarasi & Dhanya, 2016; Nageswararao et al., 2019; Sharma et al., 2022; Phawa et al., 2022). The data for rainfall and temperature was downloaded from 1951-2020, transformed into raster stacks and spatially interpolated to the groundwater well locations using the bilinear interpolation method with the help of R packages "raster" (Hijmans et al., 2015) and "sp" (Pebesma et al., 2012). For potential evapotranspiration (PET) estimation, we used the Hargreaves method (Hargreaves and Samani, 1985). While this method requires only temperature data (maximum and minimum), which are the only meteorological observations available other than precipitation, it is a simple method that can produce excessive day-to-day variability. We also tested the Penman-Monteith equation using the available observed meteorological variables (minimum and maximum temperature), latitude and elevation data and derived estimates of net solar radiation, wind speed, saturation vapor pressure and actual vapor



pressure. However, this produced implausibly low PET values (i.e., in the range of 0.88-1.88 mm/day) for the region and was hence rejected. Overall, the implications of using the Hargreaves method on the findings are, however, likely to be modest. This is because, as detailed below, the groundwater time-series modeling only uses PET in the estimation of recharge, which is then smoothed through a convolution to estimate the groundwater head. The excessive day-to-day PET fluctuations from the Hargreaves method are subsequently heavily smoothed via convolution in the groundwater response.

2.3 Time series groundwater modelling

The groundwater head hydrograph for each groundwater well was simulated using HydroSight (Peterson & Western, 2014; Peterson & Fulton, 2019). A core feature is the time-series convolution modeling whereby the observed head at any time point is simulated as the numerical integral of a weighted driver, such as rainfall. Specifically,

$$H_{sim,t} = \int_{\tau=0}^{-\infty} F(t-\tau)\Theta(\tau) d\tau \quad (1)$$

where H_t is the simulated head at time t , $F(t-\tau)$ is a driver of the head at τ days prior to t and $\Theta(\tau)$ is a weighting function for the forcing. Following Peterson and Western (2014), the forcing was the simulated daily free-drainage from a vertically lumped one-dimensional soil moisture model, effectively transforming input daily climate data into a free-drainage signal conceptualized as a gross recharge (i.e. excluding phreatic ET). The two daily climate inputs are precipitation (P) and potential evapotranspiration (PET). The soil moisture store (SMS) model can take many forms, and here a one-layer and a two-layer model were examined. Following Peterson and Western (2014), the one-layer soil moisture was modeled by solving an ordinary differential equation for the mass balance:

$$\frac{dS}{dt} = P_{inf} \left(1 - \frac{S}{SMSC}\right)^\alpha - k_{sat} \left(\frac{S}{SMSC}\right)^\beta - PET \left(\frac{S}{SMSC}\right)^\gamma \quad (2)$$

where S is the soil moisture (as a depth) in the shallow stores respectively at time t , $SMSC$ is the soil moisture capacity, P_{inf} is the daily precipitation infiltrated at time t , PET is the daily potential evapotranspiration at t , k_{sat} is the vertical saturated hydraulic conductivity and α , β , and γ are the power terms controlling the non-linearity in the infiltration, recharge and evapotranspiration, respectively. Here, the infiltration parameter (α) was fixed to 1, which implies that as the soil layer wets up, the infiltration declines, and at saturation, all precipitation goes to runoff.

The two-layer model is identical to the one-layer model, but it has a second deeper soil store whereby the free drainage from the upper store drains into the deeper store, the ET demand is first supplied by the upper store, and the deep store supplies the remaining demand. The deeper layer model was modeled using the Eq. (3):



$$\frac{dS_{deep}}{dt} = k_{sat} \left(\frac{S}{SMSC} \right)^{\beta} - k_{sat,deep} \left(\frac{S_{deep}}{SMSC_{deep}} \right)^{\beta_{deep}} - \left(PET - \left(\frac{S}{SMSC} \right)^{\gamma} \right) \left(\frac{S_{deep}}{SMSC_{deep}} \right)^{\gamma} \quad (3)$$

Here, S and S_{deep} are the soil moisture in the shallow and deeper stores respectively at time t , $SMSC$ and $SMSC_{deep}$ are the soil moisture capacity in the shallow and deeper soil stores respectively, $k_{sat, deep}$ is the vertical saturated hydraulic conductivity for the deeper soil store and β_{deep} and γ_{deep} are the power terms controlling the non-linearity in the recharge and evapotranspiration, respectively.

260 In addition to the above-discussed one-layer and two-layer soil store models, the Peterson & Fulton (2019) extension was adopted to constrain the average simulated soil evapotranspiration to a plausible range, resulting in more realistic recharge estimates. Specifically, upper and lower plausible bounds on the modelled actual ET were obtained from probabilistic estimates of the Budyko curve (Greve et al., 2015) using the aridity at the groundwater well. Any model parameter set that exceeded these constraints
265 during the calibration were rejected.

Overall, four model configurations were applied to each groundwater well, namely, one-layer ET-unconstrained SMS model (l_1v_1), two-layer ET-unconstrained SMS model (l_2v_1), one-layer ET-constrained SMS model (l_1v_2), and two-layer ET-constrained SMS model (l_2v_2).

The recharge is then weighted with a modified Pearson type III distribution function (Eq. 4):

$$\Theta(t) = A \frac{t^{n-1} \exp(-bt)}{\left(\frac{n-1}{b} \right)^{n-1} \exp(1-n)} \quad (4)$$

270 Here, A , b and n are non-physical parameters used in calibration. Specifically, A is a scaling parameter, linked to the amplitude of groundwater head response, b controls the decay rate of the weighting function, and n is the shape parameter governing the form of distribution. In the convolution equation Eq. 1, $\Theta(\tau)$ modulates the impact of $F(t-\tau)$ on $H_{sim,t}$. Essentially, it acts as a filter that determines how much the past recharge contributes to the groundwater head and the temporal structure of the system's
275 memory, i.e., whether the system has a short memory (rapid decay) or a long memory (slow decay). The convolution model allows for diverse system behaviors based on the parameters of the weighting function $\Theta(\tau)$. In a short memory response, where the decay parameter b is large, the influence of recharge diminishes rapidly, causing the system to respond quickly to rainfall with minimal lasting effects. Conversely, a long memory response arises when decay factor b is small, resulting in a gradual
280 attenuation of recharge impacts over extended periods. This reflects systems where past recharge continues to affect groundwater levels for years or even decades.

A large time lag between recharge and head response is observed when the shape parameter n increases. This causes $\Theta(\tau)$ to peak at longer time lags, indicating delayed head responses, often due to slow



propagation in thick unsaturated zones or low-permeability aquifers. Different combinations of
285 parameters (A, b, n) can yield complex behaviors, such as a strong immediate response with slow decay
or minimal short-term impact with prolonged influence. These outcomes allow the model to represent
a wide range of hydrogeological scenarios, from shallow, rapidly draining systems to deep aquifers with
significant storage capacity.

2.3.1. Model calibration

290 To achieve the best fit for the model to an observed hydrograph, each model was calibrated using the
global calibration scheme Covariance Matrix Adaptation Evolution Strategy (CMA-ES) (Hansen,
2006). Each one-layer model has seven parameters to calibrate, with soil moisture capacity (SMSC),
vertical soil conductivity (k_{sat}), drainage parameter (β) for the SMS model and three parameters from
the Pearsons' Type III distribution weighting function (A, b, n) and the exponential noise function (μ).
295 In the case of a two-layer model, deep layer soil moisture capacity (SMSC_{deep}) and potential
evapotranspiration parameter (γ) are also calibrated for the SMS model, thus making a total of nine
parameters for calibration. The calibration uses an approximate likelihood negative log objective
function, which evaluates the fit of the model to observed data. By minimizing this objective
function, the CMA-ES algorithm adjusts the model parameters to maximize agreement between observed and
300 simulated hydrographs. The calibration population size was set to eight times the number of model
parameters, and the convergence criteria for the objective function was 1×10^{-8} .

Each groundwater model was calibrated over four observation lengths. Firstly, the total observation
record was used. We then tested the predictive skill of each model. For this, we employed a split
sampling approach and tested the model prediction performance over different time periods. Based on
305 the length of groundwater head time series records of the 92 groundwater wells, we selected the last 2,
4 and 8 years to test the model's ability to predict groundwater trends under different timescales. A
shorter evaluation period (e.g., 2 years) allows for more calibration data, improving model reliability
but capturing only short-term climate influences. As the evaluation period extends to 4 and 8 years, the
prediction window increases, providing a better assessment of long-term climate effects. However, this
310 comes at the cost of reduced calibration data, potentially increasing uncertainty. This approach helps
balance predictive accuracy and data availability, ensuring confidence in identifying climate-dominated
groundwater responses.

2.4 Identification of climate-dominated groundwater wells

2.4.1. Calibration period

315 After calibrating each groundwater well, the fit to the calibrated period was examined to assess if this
provides an adequate identification of climate-dominated groundwater wells - as others have relied on.
We considered two criteria:



- i. The goodness of fit of the hydrograph. For a well to be identified as climate-dominated, the simulated head over the calibration period should be unbiased and approximately reproduce the observed variability and timing of fluctuations. Following others (Shapoori et al., 2015a and Fan et al., 2023), here we use the standard Coefficient of Efficiency (CoE) (Eq. 5) (Nash & Sutcliffe, 1970):

$$CoE = 1 - \frac{\sum_{t=1}^N (H_{obs,t} - H_{sim,t})^2}{\sum_{t=1}^N (H_{obs,t} - \bar{H}_{obs})^2} \quad (5)$$

Where N is the duration of the calibration period, H_{obs} and H_{sim} are observed and simulated groundwater heads at time t , \bar{H}_{obs} is the mean of observed groundwater heads for the total duration N . The CoE values range from $-\infty$ to 1, where 1 indicates a perfect fit and 0 indicates a fit no better than obtained from the observed mean head. While a $CoE \geq 0.80$ is commonly referenced in hydrological modelling as a good predictive skill score, particularly in surface water (Moriassi et al., 2007; Ladson, 2008), groundwater time series model can exhibit extremely high CoE values because of strong serial correlation in groundwater head time series, but also very low values because of the absence of a fixed lower bound. For example, Fan et al. (2023) adopted a CoE of 0.8 to identify climate-dominated sites. Although the study puts a threshold of $CoE \geq 0.8$ for identifying climate-dominated sites, a lower CoE score (i.e., 0.6-0.8) still indicates that the model captures the dominant climate fluctuations. Here, we adopted a calibration CoE threshold of 0.6 to delineate climate-dominated groundwater wells.

- ii. The partitioning of the rainfall must be plausible. As discussed above, the internal plausibility of the model dynamics is often not considered when denoting a site as climate-dominated or otherwise. Here, we estimated the recharge coefficient, which is calculated as the ratio of the mean drainage to mean rainfall. For semi-arid to arid regions, the ratio is understood to be low due to limited precipitation and high evapotranspiration rates.

2.4.2. Evaluation/prediction period

To assess the prediction performance of the model during the evaluation period, we first evaluated using standard CoE. However, groundwater hydrograph simulations can exhibit different combinations of bias and variability that are not always clearly distinguished by CoE alone. This behaviour is illustrated conceptually in Fig. 2.

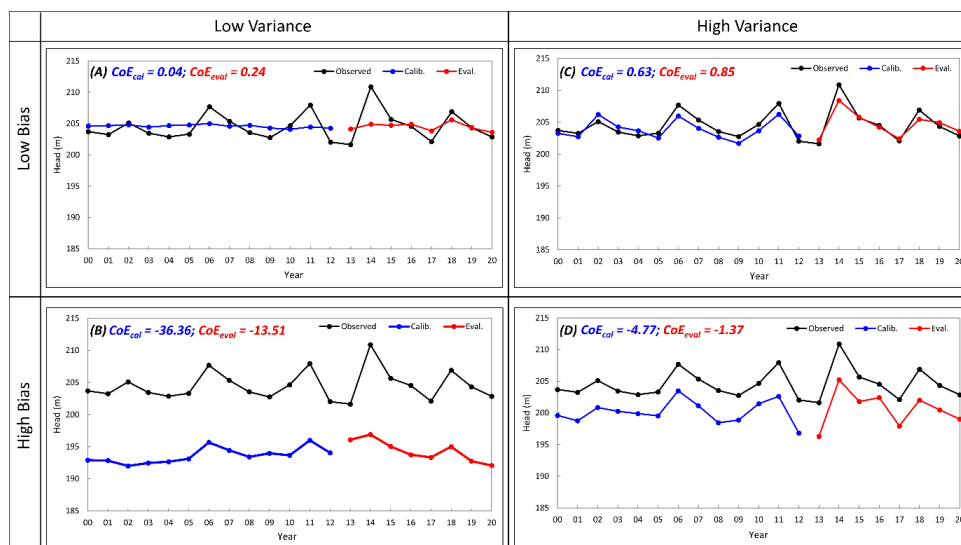
We identify four broad outcomes that can arise when comparing simulated and observed groundwater heads. Model A (Fig. 2A) and Model C (Fig. 2C) represent cases of low bias, where the mean simulated groundwater head aligns closely with observations. However, Model A exhibits low variance and fails



350 to capture observed variability, whereas Model C reproduces both the mean behaviour and the observed variability. In contrast, Model B (Fig. 2B) and Model D (Fig. 2D) represent cases of high bias, where simulated groundwater heads deviate substantially from observations, while still differing in their ability to reproduce observed variability. Model B underrepresents variability, whereas Model D captures observed fluctuations more accurately despite the presence of systematic bias.

355 When evaluated using CoE, these contrasting behaviours can lead to ambiguous performance rankings. While Model C is correctly identified as the best-performing simulation, models that reproduce long-term trends but fail to capture variability may receive higher CoE values than simulations that capture variability well but exhibit constant bias.

360 From a groundwater evaluation perspective, simulations that reproduce observed variability are often more informative for understanding system dynamics and driver influence than simulations that reproduce mean groundwater levels alone. This illustrates a limitation of relying solely on CoE for evaluating groundwater model performance during prediction and attribution analyses.



365 **Figure 2: Conceptual diagram of four possible groundwater head modelling scenarios over a calibration and evaluation period. The columns examine high and low simulated variance scenarios and the rows high and low bias scenarios (A) Low bias and low variance. (B) High bias and low variance. (C) Low bias and high variance. (D) High bias and high variance.**

To address this, we introduce three additional performance metrics that modify the standard CoE formula to account for both bias and the ability to capture trends, ensuring a more hydrologically relevant model evaluation tested during the evaluation periods. Additionally, we adopted a technique from ensemble forecasting, specifically Continuous Ranked Probability Score (CRPS), to account for the predictive uncertainty.

370



Equation (5) is used for the standard CoE for the evaluation period, and further modifications have been made to introduce our three new performance metrics. The second performance metric is the unbiased coefficient of efficiency (CoE_μ) (Eq. 6). The key modification here is that we subtract the mean residual from each residual before squaring. This removes any systematic bias in the model predictions.

The third performance metric is the standard coefficient of efficiency but extended to use the total observed variability over the entire observation record (CoE_σ) (Eq. 7). Normally, CoE is affected by changes in variability between these periods. If the evaluation period has greater variability than the calibration period—perhaps due to a shorter record or altered drives such as pumping—CoE reduces, even if the model’s error spread remains similar. To address this we adjusted Eq. (5) by normalizing the errors using the total observed variability over the full dataset rather than just the evaluation period. The equation thus helps to stabilize the model performance evaluation, making comparisons across different periods more reliable, even when the hydrological conditions change.

The fourth performance metric is the unbiased coefficient of efficiency for total observed variability (CoE_{μ,σ}), which is the hybrid of the above two metrics (Eq. 8). It combines the benefits of bias correction and normalization by total variability and ensures that both systematic biases and the model’s ability to replicate the entire range of observed data (from short-term fluctuations to long-term trends) are accurately assessed.

$$CoE_{\mu} = 1 - \frac{\sum_{t=1}^n \left((\overline{H_{obs} - H_{sim}}) - (H_{obs,t} - H_{sim,t}) \right)^2}{\sum_{t=1}^n (H_{obs,t} - \overline{H_{obs}})^2} \quad (6)$$

390

$$CoE_{\sigma} = 1 - \frac{\sum_{t=1}^n (H_{obs,t} - H_{sim,t})^2 \times N}{\sum_{t=1}^N (H_{obs,t} - \overline{H_{obs}})^2 \times n} \quad (7)$$

$$CoE_{\mu,\sigma} = 1 - \frac{\sum_{t=1}^n \left((\overline{H_{obs} - H_{sim}}) - (H_{obs,t} - H_{sim,t}) \right)^2 \times N}{\sum_{t=1}^N (H_{obs,t} - \overline{H_{obs}})^2 \times n} \quad (8)$$

Here, n is the number of observations of the evaluation period, N is the number of observations for the complete record, and $\overline{H_{obs}}$ is the mean of observed groundwater head for the total evaluation period n.

While the CoE variants—CoE_μ, CoE_σ, and CoE_{μ,σ}—were introduced to address bias and variance limitations of the standard CoE, they remain fundamentally point-based metrics that summarize performance using aggregated squared errors. While CoE_μ removes systematic bias and CoE_σ adjusts for changing variance, yet they do not assess how variability is distributed over time. Even CoE_{μ,σ}, which combines both corrections, does not evaluate how well the model captures the temporal structure



of observed fluctuations. However, all four CoE metrics ignore predictive uncertainty, despite
400 uncertainty being an important component of groundwater head prediction and driver attribution. This
raises an important question: how should we compare two models that are both biased, but one has low
uncertainty while the other has high uncertainty? A model with narrow predictive intervals may appear
more accurate but often misses observations, while another with a greater uncertainty may more reliably
include them. In contrast, the latter—though associated with greater uncertainty—offers a more reliable
405 and transparent representation of model performance. This highlights the need for evaluation
approaches that consider both accuracy and predictive uncertainty to ensure a more meaningful
assessment of model performance.

One approach to address this is adopting metrics developed to evaluate probabilistic forecasts. Unlike
deterministic metrics, probabilistic metrics account for prediction uncertainty and hence offer a more
410 comprehensive assessment of model reliability (Krzysztofowicz, 2001). Despite their extensive
application in surface water modeling, probabilistic approaches remain largely unexplored in
groundwater studies – possibly, we speculate, because predictive evaluation receives less attention in
groundwater than surface water studies. Here, we adopt the Continuous Ranked Probability Score
(CRPS) method from ensemble forecasting as our fifth metric. CRPS evaluates the entire predicted
415 cumulative distribution function (CDF) at each time step against the observations, thereby assessing
both prediction accuracy and the associated uncertainty (Gneiting & Raftery, 2007). Mathematically,
the CRPS for a predicted CDF $F(y)$ and an observed value x is defined as:

$$CRPS(F, x) = \int_{-\infty}^{\infty} (F(y) - \mathbb{1}(y - x))^2 dy \quad (9)$$

$$\text{where } \mathbb{1} \text{ is the Heaviside step function } \mathbb{1}(x) = \begin{cases} 0, & \text{for } x < 0 \\ 1, & \text{for } x \geq 0 \end{cases} \quad (10)$$

420

The CRPS values are computed using the ‘*scoringRules*’ package in R (Jordan et al., 2017). Further, as
the CRPS computation is performed for each timestep, here we calculate the mean CRPS over an
evaluation period. Additionally, to enable comparison between groundwater wells with very different
variability in the observed head, we normalize the average CRPS by the standard deviation of the
425 observed head.

$$CRPS = \frac{1}{T} \sum_{t=1}^T CRPS_t \quad (11)$$



$$CRPS_{ratio} = \frac{CRPS}{SD_{obs}} \quad (12)$$

The CRPS ratio values range from 0 to ∞ , where low values (closer to 0) indicate accurate prediction and higher CRPS (greater than ~ 1) indicate poor predictive performance. A CRPS ratio of 1 indicates that the prediction error is of a similar magnitude to the variability in the observed data.

To evaluate the metrics across the groundwater wells, we construct scatter plots of the calibration period CoE against each evaluation period performance metric. For this, thresholds of calibration $CoE \geq 0.2$ and evaluation $CRPS \leq 0.8$ are used to classify wells with climate influence and reasonable predictive reliability. Here a low calibration CoE criteria was adopted to place the most weight on the evaluation performance while allowing rejection of the occasional well that is well simulated during only the evaluation period. Now, to interpret these plots, the plot space is divided into four quadrants. The reasoning for this is that if a groundwater well is truly dominated by climate, then it should be plotted in a region that has good calibration and evaluation performance. Similarly, if another driver (e.g. groundwater pumping) dominates over the entire record, then performance should be poor over both calibration and evaluation and hence, it should plot in the diagonally opposite quadrant. However, if other drivers emerge only during the calibration or evaluation periods, then they will plot on the opposite diagonal axis. Most interestingly, if groundwater pumping occurred only during the evaluation periods, then this approach would avoid the false positive identification of it as climate-dominated – if one relied only on the calibration performance. By applying the quadrant approach, we are able to visually and quantitatively identify and classify wells based on their placement in each quadrant and link them with the likely driver of influence on the groundwater head. Further, we then examined the spatial continuity of the performance metrics across the study area.

3 Results

3.1 Calibration period identification of climate-dominated wells

The identification of climate-dominated groundwater wells has very often been assessed using the fit to the observed hydrograph over the calibration period. Here we start with this approach. Fig. 3 summarizes the CoE performance during the calibration period for all four model types. Using the criterion of $CoE \geq 0.60$, the ET-unconstrained one-layer and two-layer models (i.e., I_1V_1 and I_2V_1) identified 24% ($n=22$) and 20% ($n=18$) of groundwater well locations as climate-dominated, respectively. Interestingly, 17 of the two-layer model wells were also identified by the one-layer model. This consistency is encouraging but suggests that a one-layer model may be more likely to produce false positive identification of climate-dominated wells.

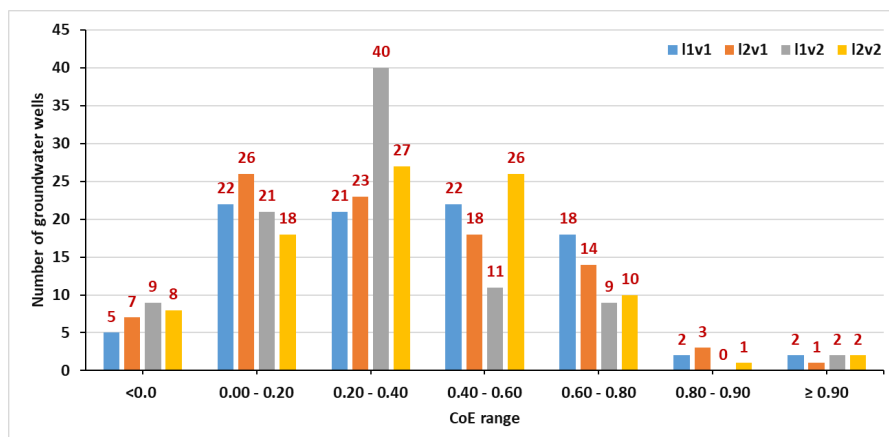


Figure 3: CoE performance summary of 92 groundwater wells evaluated for four models over a full calibration period

460

On applying the ET constraint in the model structure, the results of the one-layer (l_1v_2) and two-layer (l_2v_2) models show 12% ($n=11$) and 14% ($n=13$) of the groundwater well locations to be climate-dominated, respectively. Four groundwater well locations (25, 70, 77, and 83) were identified as climate-dominated in both the one-layer and two-layer ET-constrained models.

465

Fig. 4 maps the calibration CoE at each well from each of the four model structures. It shows that for all four models, the climate-dominated (with $CoE \geq 0.60$) wells are primarily in the eastern part of the region (i.e., on and around the borders of the Aravalli and Sabarkantha district) and in small clusters/patches in the northern part of the Banaskantha district, in the center of the region (i.e., on the borders of Patan, Mehsana and Banaskantha district) and the southern tip of the Mehsana district. The mid-range CoE values (0.4-0.6) also populate around these spots around the climate-dominated groundwater wells. The low CoE values ≤ 0.2 appear primarily in the western parts of the region (i.e. Banaskantha and Patan districts) and are scattered over the central part of the region. This spatial consistency across the models is encouraging, considering each groundwater well was analyzed independently. Overall, they suggest that wells in the east appear likely to be climate-dominated, and

470

as we move towards the west, we see climate-dominated wells becoming less common and scattered or in small patches. However, this assessment ignores the plausibility of the modeled dynamics and predictive skills.

475

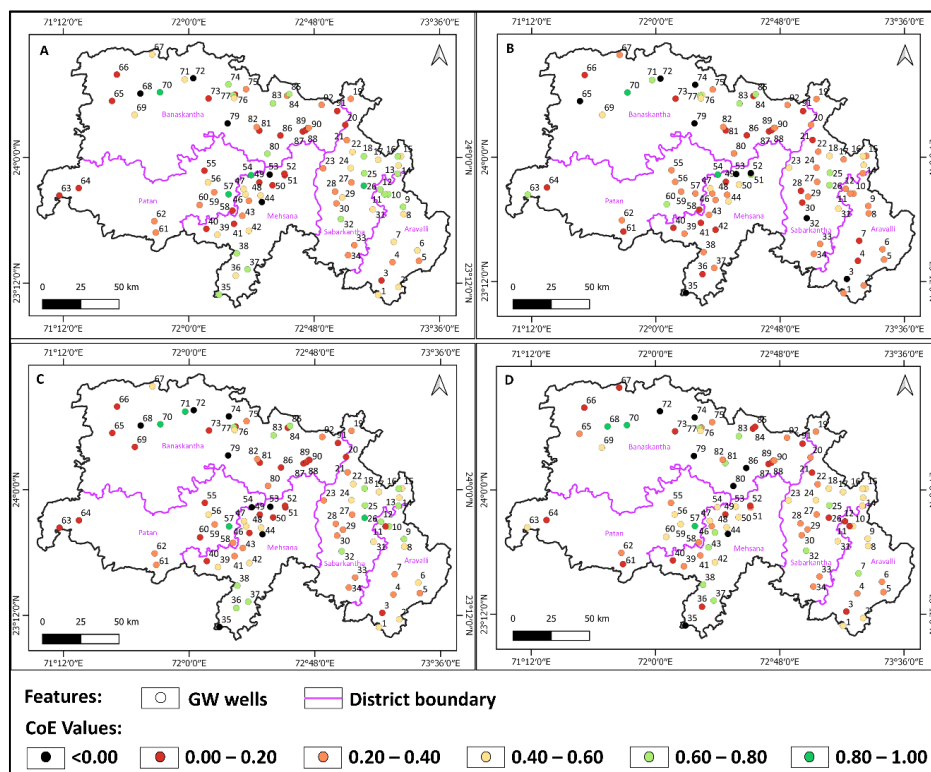


Figure 4: Calibration period CoE for 92 groundwater well locations across the North Gujarat region evaluated for (A) One-layer ET-unconstrained model (l_{1v1}). (B) Two-layer ET-unconstrained model (l_{2v1}). (C) One-layer ET-constrained model (l_{1v2}). (D) Two-layer ET-constrained model (l_{2v2}).

480

3.2 Are the recharge estimates plausible?

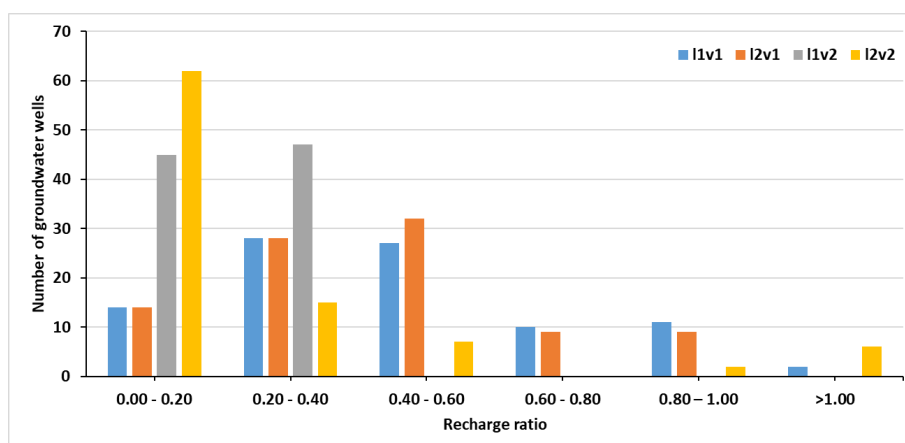
The calibration CoE shows that the groundwater head in the east is likely to be climate-dominated. To examine if such good model performance also aligns with plausible internal model dynamics, and hence we can have more confidence in them, we further evaluated the recharge estimates produced by the models. Fig. 5 summarizes the recharge-to-precipitation (R/P) ratio for each of the four models for the 92 groundwater wells. The ET-unconstrained models tend to overestimate recharge, leading to unrealistically high R/P ratios in many wells. Taking a 20% threshold for annual recharge, only 15% (n=14) of wells from these models fall below this limit—far fewer than expected. This overestimation occurs because the model is not able to handle the proper partitioning of rainfall, sending too much to recharge instead of evapotranspiration.

490

In contrast, the ET-constrained models produce a more realistic distribution of recharge estimates. Here, 50% (n=46) and 67% (n=62) of wells, in one-layer and two-layer models, respectively, show annual



495 recharge below 20%, suggesting that incorporating ET constraints prevents excessive recharge and maintains a more balanced water partitioning. Among these, the one-layer ET-constrained model appears to perform best, producing a spatially correlated pattern of climate-dominated wells while maintaining hydrological consistency.



500 **Figure 5: Recharge ratio summary of 92 groundwater wells evaluated for four models over a full calibration period**

The spatial distribution of recharge further reinforces these findings (Fig. 6). In the ET-unconstrained models, recharge rates below 20% were confined to small patches, mainly in the Banaskantha district, along the Patan-Mehsana border, and in the Aravalli district. Meanwhile, recharge rates exceeding 40% were widespread, covering all districts. In stark contrast, the ET-constrained models presented the opposite pattern: recharge rates below 20% were spread across the entire region, while recharge rates exceeding 20% were largely concentrated around the Mehsana-Patan border. This pattern aligns better with the region’s hydro-meteorological conditions and land use, suggesting that the ET-constrained models provide more realistic recharge estimates.

510 That said, some ET-constrained models still exhibit higher-than-expected R/P ratios, even when they meet the CoE threshold. This can occur when a high initial soil water storage rapidly drains and artificially inflates recharge estimates. This highlights a key limitation of relying solely on calibration performance: a good model fit does not always mean the underlying processes are realistic. For this reason, we focus our subsequent analyses on the ET-constrained models, which offer a more physically plausible representation of groundwater recharge.

515

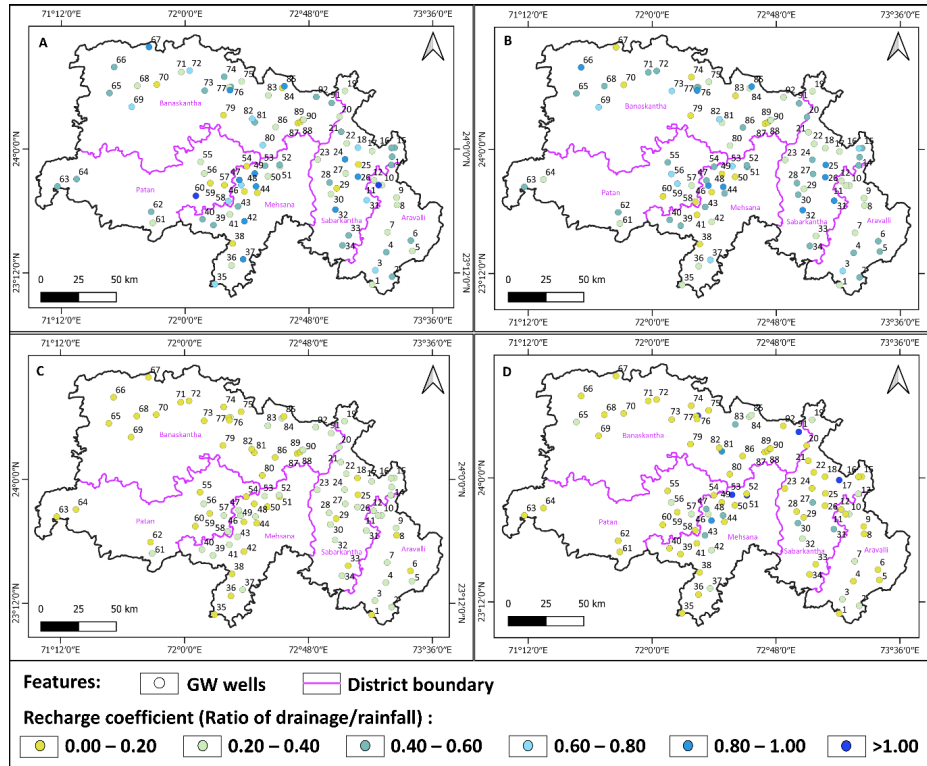


Figure 6: Distribution of recharge coefficient values for 92 groundwater well locations across the North Gujarat region evaluated for (A) One-layer ET-unconstrained model (I_{1V1}). (B) Two-layer ET-unconstrained model (I_{2V1}). (C) One-layer ET-constrained model (I_{1V2}). (D) Two-layer ET-constrained model (I_{2V2}).

520

3.3 Predictive performance of the models

The assessment of the model internal dynamics showed that only those models with ET constraint produced plausible recharge. Henceforth, we only examine the ET-constrained models.

To illustrate the relationship between the model predictions and the five performance measures, Figs. 7 and 8 show six observed, calibrated and predicted hydrographs for two performance metrics. To illustrate the assessment of calibration and evaluation results, a scatter plot of performance is divided into four quadrants using two thresholds

Fig. 7 shows the $CoE_{\mu,\sigma}$ metric against the CoE_{cal} for the 4-year evaluation period. The hydrograph for groundwater well 31 (Fig. 7D) shows a good fit between observed and simulated groundwater heads during both calibration and evaluation periods, with the seasonal and long-term trend well simulated. Thus, the model effectively simulates groundwater dynamics with minimal bias and a high degree of explained variance. Both performance metrics are hence high, so the well plots in the top right quadrant.

530

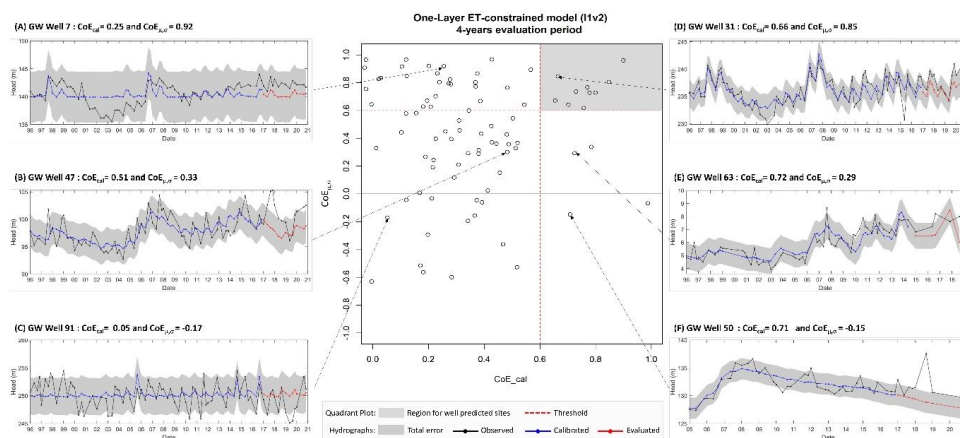


Given that the variability over both periods is explained using only climate forcing, this well is unlikely to be substantially influenced by other drivers, such as groundwater pumping.

535 In a somewhat similar context, Well 63 (Fig. 7E) shows a good fit over the calibration period, and the model can capture much of the observed trend in the evaluation period. Hence, this well plots in the top right quadrant but outside of the region of likely climate dominated performance, possibly because of an unaccounted external driver.

Looking at the diagonally opposite quadrant, at well 91 (Fig. 7C) the seasonal dynamics during both
 540 periods could not be simulated using only climate data. Hence, the well is likely to be influenced by a driver(s) other than only climate. Moving towards the top-left quadrant, the calibration of well 47 (Fig. 7B) was adequate but the evaluation period is clearly biased and has low variance. Since the bias was not removed, the evaluation score is poor and hence the wells plots in the top left quadrant. Therefore, the evaluation performance is insufficient to classify the well as being driven only by climate. Similarly,
 545 well 7(Fig. 7A) also plot in the top left and shows a poor fit, particularly during the calibration period. However, the high evaluation score (0.92) is difficult to reconcile with the poor graphical results, which compromises confidence in the $CoE_{\mu,\sigma}$ metric.

Lastly, in the bottom right quadrant, well 50 (Fig. 7F) is dominated by a multi-year trend, overlain with intra-year variability. The simulation does capture the multi-year trend but fails to capture the intra-year variability. Given the high observed variance, the poor intra-year predicted variability is heavily
 550 penalized by the $CoE_{\mu,\sigma}$, resulting in this well being identified as not climate dominated. If only the calibration CoE was used to categorize this well, then it would be incorrectly identified as climate-dominated.



555 **Figure 7: Performance of 92 groundwater well locations for one-layer ET-constrained model evaluated over 4 years using $CoE_{\mu,\sigma}$ against CoE_{cal}**



To demonstrate an alternate evaluation metric, Fig. 8 shows the CRPS results against the CoE_{cal} for the 4-year evaluation period. Here two groups of wells are shown: (i) Fig. 8A-C and E show wells with a CoE_{cal} of ~ 0.2 but varying CRPS; and (ii) Fig. 8D and F shows wells with a CoE_{cal} of ~ 0.4 but, again, a varying CRPS. On the latter, well 22 (Fig. 8F) closely matches observed during both periods with little bias and CRPS correspondingly shows a low prediction error. In contrast, well 43 (Fig. 8D) has a similar CoE_{cal} but the prediction is biased. The CRPS appropriately captures this poorer predictive skill. Looking at the former group with a CoE_{cal} of ~ 0.2 , the predictive skill spans from poor at well 42 (Fig. 8A) to very good at well 76 (Fig. 8C). Encouragingly, the CRPS score appropriately improves with the graphical results such that well 42 has a high error of 1.155, wells 1 and 4 have a CRPS of 0.84 to 1 and well 76 has the lowest CRPS of 0.7. Looking across these two groups, wells 22 and 76 both have a lower CRPS of ~ 0.7 but the former has a better CoE_{cal} of ~ 0.4 . However, visually the two simulations are comparable. This suggests that CoE_{cal} is not a strong discriminator of model performance and, in light of the strong performance of CRPS, that CRPS appears to more reliably identify those wells as likely to be climate dominated.

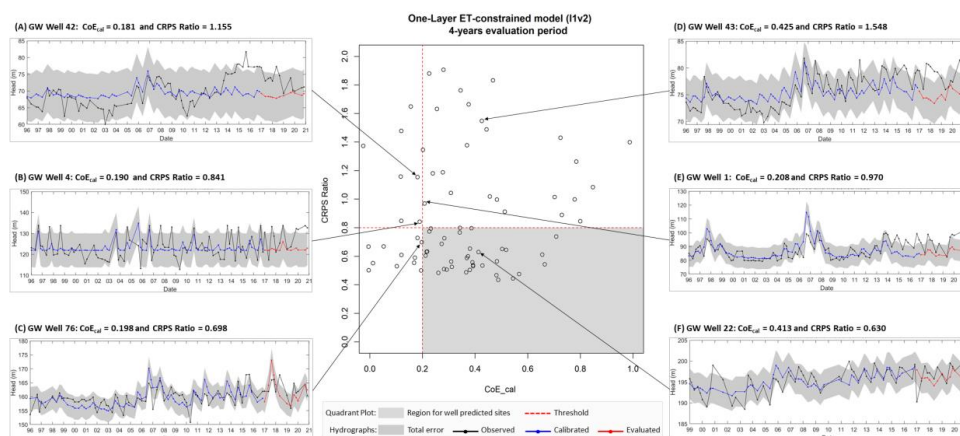


Figure 8: Performance of 92 groundwater well locations for one-layer ET-constrained model evaluated over 4 years using CRPS ratio against CoE_{cal}

To examine all evaluation metrics across different prediction durations, Fig. 9 shows scatter plots for 2-year, 4-year, and 8-year evaluation periods using the five performance metrics. All 92 selected groundwater wells were included in each evaluation period analysis, and no wells were excluded from the longer evaluation periods. To assess how well these metrics distinguish climate-dominated from pumping-dominated wells, we consider two key factors. First, land-use changes in the study region have been minimal over the past two decades, as confirmed through visual inspection of historical satellite imagery on Google Earth and comparison of land use statistics from Bhuvan-NRSC datasets (2005–06 to recent years), indicating that water use patterns have remained relatively stable. This suggests that



the dominant drivers influencing groundwater heads have remained relatively consistent between the calibration and evaluation periods. Second, field observations provide insights into wells affected by groundwater pumping or climate based on their location and purpose, as discussed in Section 4.

585 Considering these factors, we expect truly climate-dominated wells to exhibit consistency between calibration and evaluation metrics. A well significantly influenced by pumping during calibration (low calibration metric score) should also perform poorly during evaluation (low evaluation metric score), assuming persistent non-climatic influences. A robust CoE-based metric should, therefore, show a clear diagonal trend from the bottom-left to the top-right quadrant. However, several CoE-based metrics (Fig. 9A–F) fail to capture this consistency, displaying a scattered calibration-evaluation relationship. While 590 the modified CoE metrics show improved bias and variability handling (Fig. 9G–L), their inability to clearly distinguish climate-dominated wells from those affected by pumping detracts from their utility for identifying climate dominated sites. Specifically, the large number of wells plotting in the top-left quadrant suggests that the modified CoE evaluation metrics are prone to identifying sites as having an 595 additional driver (e.g. pumping) only during the calibration period. Given Fig. 9 shows this outcome is independent of the prediction length, it is implausible and hence invalidates these CoE metrics.

For CRPS (Fig. 9M–O), we expect a diagonal trend from the top-left to the bottom-right quadrant, indicating that climate-dominated wells should cluster in the bottom-right. Encouragingly, Fig. 9M shows such a strong calibration-evaluation relationship. The low number of wells in the bottom-left 600 (poor calibration but good evaluation) and top-left (poor calibration and poor evaluation) quadrants suggest that poorly calibrated wells rarely transition into well-simulated wells during evaluation. This pattern does degrade as the prediction duration increases (and calibration duration decreases) to 4 years and then to 8 years. However, overall CRPS appears to offer the most logical performance across the study region and when looking at individual hydrographs. Henceforth it is adopted to examine which 605 wells are likely to be climate dominated.

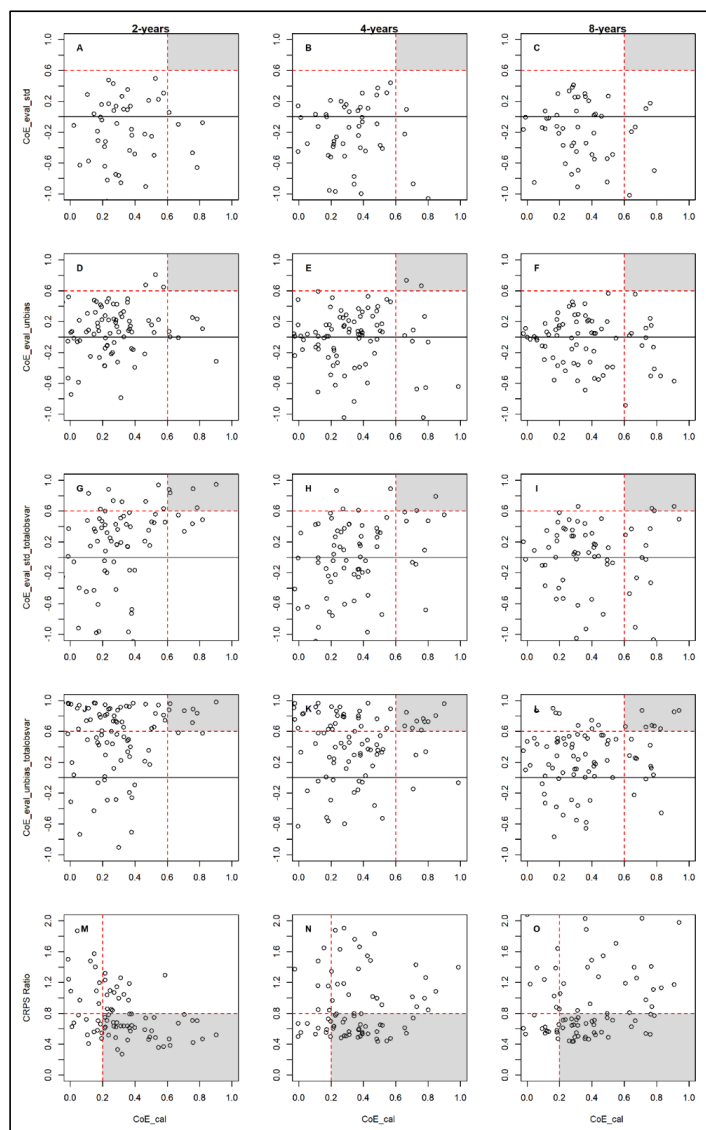


Figure 9: Quadrant plots for the one-layer ET-constrained (I_1V_2) SMS models for each groundwater well location. Each groundwater well is examined for three evaluation periods: 2 years, 4 years and 8 years, using four different CoE measures and CRPS ratio. For the CoE-based quadrant plots (A to L), climate-dominated wells are identified using a threshold of $CoE \geq 0.60$ during both calibration and evaluation. For CRPS ratio quadrant plots (M to O), climate-dominated wells are identified using a CoE calibration >0.2 and a CRPS ratio <0.8

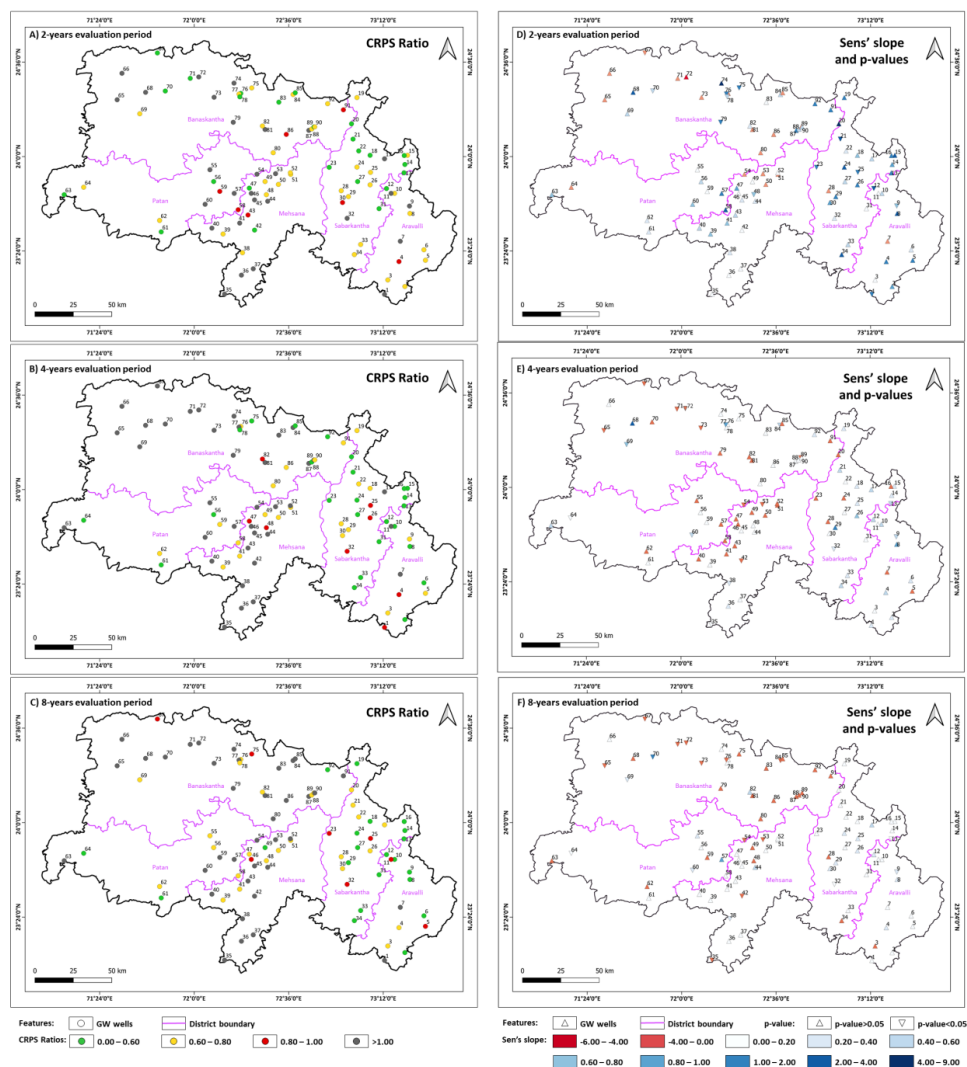
Fig. 10 (A, B, C) shows maps of the CRPS results for 2,4 and 8-year evaluation periods. It shows a consistent clustering of low CRPS wells (<0.8 and color coded in green and yellow) in the northern and



eastern regions, particularly in Banaskantha, Aravalli, and parts of Sabarkantha, more likely to be climate-dominated. Meanwhile, wells with a high CRPS (≥ 0.8 , color-coded and red and black) are concentrated in Mehsana and the western part of Banaskantha district and are unlikely to be influenced by climate. Further, as the evaluation period is increased from 2 to 8 years, the wells showing high
620 CRPS metrics reduce. Importantly, when a site appears as climate dominated across 2-, 4- and 8-year evaluation periods, we can have more confidence in the site being genuinely climate dominated.

However, this analysis only indicates whether an external driver other than climate likely to influences the groundwater level dynamics within the observation periods. To understand the possible influential non-climate drivers, the sign of the error between the observed and modeled level may be informative.
625 For example, if groundwater pumping is producing significant drawdown at the observation well, we would expect our climate-based model to overestimate the observed head, resulting in negative error residuals (observed minus modeled head). Additionally, we expect that increased pumping over time to result in more negative residuals over time, resulting in a statistically significant negative slope with time. Conversely, a positive residual slope suggests the presence of an external driver that increases the
630 groundwater head, such as canal seepage or traditional recharge structures.

Using this logic, Figs. 10 (D, E, F) show the spatial distribution of Sen's slope and p-values for residuals over different evaluation periods (2, 4, and 8 years). Negative slopes (shades of red) are particularly concentrated in Mehsana and the western part of Banaskantha, indicating areas where groundwater depletion is occurring beyond what climate alone can explain. Meanwhile, positive slopes (shades of
635 blue) are predominantly observed in the eastern districts, particularly Sabarkantha, suggesting external recharge mechanisms at play. By correlating these trends with CRPS metrics and p-values, the results suggest that groundwater wells classified as non-climate dominated—notably in western Banaskantha and central Mehsana—are likely to be influenced by groundwater pumping. In contrast, the eastern side of North Gujarat appears climate-dominated, where observed groundwater heads align more closely
640 with climate variability. Interestingly, in the central-southern part of the region—particularly along the Mehsana–Patan border—some wells classified as non-climate dominated show a positive residual trend, suggesting the influence of land cover changes or interventions that enhance recharge. This aligns with the presence of major canal systems in the area, including the Dharoi and Narmada canal networks, as well as the widespread construction of check dams on local rivers, which may be contributing to rising
645 groundwater heads in these semi-arid zones.



650 **Figure 10: Spatial maps representing CRPS ratios for 92 groundwater wells for ET-constrained one-layer model (11v2) evaluated over (A) 2-years period; (B) 4-years period; (C) 8-years period and p-value for the residuals (observed-modelled), where a negative slope suggest an extractive driver, e.g. pumping) for 92 groundwater wells for ET-constrained one-layer model (11v2) evaluated over (D) 2-years period; (E) 4-years period; (F) 8-years period**



4 Discussions

Previous groundwater attribution studies have relied on calibration fit to identify climate-dominated groundwater well and have not accounted for the predictive performance. Here, we examined the adequacy of this approach by evaluating both the calibration and prediction performance using a combination of standard and newly adapted performance metrics. We applied these analyses to 92 groundwater wells across the North Gujarat Region in western India using the HydroSight and examined five evaluation metrics, four based on the widely used coefficient of efficiency and a fifth on a variance scaled form of the continuous ranked probability score (CRPS).

Given that others have relied only upon the calibration performance, we started from the same approach. Our results showed that for the full-period calibration, CoE values having a threshold of ≥ 0.60 from all four models suggest that the eastern region of North Gujarat (i.e., the Aravalli and Sabarkantha districts) appears to be climate-dominated. In contrast, as we move westward towards Patan and Banaskantha districts, climate-dominated groundwater wells become less common and appear in smaller, scattered patches. To examine the veracity of these findings, we further evaluated the models by testing their predictive skill over 2-, 4-, and 8-year periods.

Before doing so, we also examined the plausibility of the internal model dynamics to eliminate models that conflict with independent observations. Our results show that ET-unconstrained models tend to overestimate recharge, leading to unrealistically high recharge-to-precipitation (R/P) ratios. In contrast, ET-constrained models yield more realistic recharge estimates (0–20%), aligning well with independent studies using tracer techniques (Sukhija and Shah, 1976; Sukhija et al., 1996), water table fluctuation and chloride mass balance methods (Sharda et al., 2006), and empirical approaches (Mistry and Suryanarayana, 2021). Overall, these findings evidence the risk of relying only on calibration fit.

On the predictive skill, the five performance metrics were applied to three evaluation durations (2, 4 and 8 years) and graphically compared with the calibration CoE. Looking at the individual wells, the CoE based prediction metrics often produced scores inconsistent with the graphical evaluation. However, all CoE-based metrics suggested that drivers other than climate emerged during the evaluation periods, and that this implausibly changed with the evaluation length. Overall, these findings suggest that the evaluation period CoE is an inappropriate metric to identify climate-dominated wells, and the estimations presented in previous studies by Fan et al. (2023) and Wunsch et al. (2022) may also have implications, as they relied primarily on calibration period performance for groundwater driver attribution.

In contrast, the CRPS metric provided strong evidence for distinguishing climate-dominated wells from those influenced by external drivers, offering both spatial and temporal consistency in groundwater dynamics. Spatially, CRPS effectively captured regional contrasts, with lower values clustering in the eastern and northern districts, where groundwater fluctuations closely followed climate variability, and



higher values in the western and central regions, where anthropogenic influences are more pronounced. Temporally, as the evaluation period extended from 2 to 8 years, high CRPS values became less frequent. This increases confidence in sites identified as climate-dominated across multiple evaluation periods. When combined with residual slope analysis, CRPS further strengthened its diagnostic capability. Of those wells identified as not climate-dominated, the slope of the residuals suggests that wells in the western region are likely influenced by groundwater pumping while the those in the center-south are likely influenced by land cover changes, such as drainage canals, that increased recharge. That said, this analysis identifies only the net influence of drivers and wells could be plausibly influenced by all three drivers.

Overall, CRPS suggests that between 51% (n=47) to 37% (n=34) of groundwater wells are climate-dominated (2 and 8 years evaluation periods, respectively). Spatially, these wells were located primarily in the eastern districts of the North Gujarat region, particularly Sabarkantha, followed by the northern parts of the Aravalli district. We also see the climate-dominated wells in patches in the eastern part of the Banaskantha district and over the Mehsana district. These wells are located in regions with less rainfall deficit (as shown in Fig. 2), and the associated land use and water availability conditions further support their classification. For instance, Wells 75 (CRPS = 0.56), 85 (CRPS = 0.47), and 92 (CRPS = 0.48) are located in built-up areas with minimal agricultural activity and limited groundwater pumping. In contrast, Well 78 (CRPS = 0.44) lies within agricultural land, approximately 750 meters from the West Banas River and within the canal command area of the Sipu Dam. The Sipu Dam has been supplying surface water for irrigation in this region since 2001, and based on field investigations and farmer interactions, agriculture here is typically practiced during the monsoon season or supported by this surface water in winter and summer—leading to reduced dependence on groundwater pumping and supporting the classification of the well as climate-dominated.

In contrast, non-climate dominated wells (CRPS ratio ≥ 0.80) are located in the western district of the North Gujarat region, particularly in the western part of Banaskantha district, which has a high rainfall deficit and hence have a greater reliance on external water sources such as groundwater (as shown in Fig. 2).

An ongoing challenge in evaluating such findings is, however, that independent evidence is often lacking given the paucity of metered groundwater usage. Therefore, here we evaluate the findings using (i) field observations of groundwater usage and land cover and (ii) government classification of groundwater extractions. On the field observations, site inspections throughout western Banaskantha showed that wells 68, 69, and 70 are significantly influenced by pumping from nearby agricultural wells. Given that these three wells were found to be not climate-dominated (CRPS of 5.08, 1.83 and 1.08, respectively), this suggests that the results aligns with the field evidence. Similarly, inspection of wells 13-16 (CRPS ratios – 0.53, 0.43, 0.52 and 0.46) in the Sabarkantha district suggested that they are not influenced by groundwater pumping. Field interactions with farmers and Google Earth imagery



analysis were used to assess land use, cropping patterns, and water source dependence at each of these
725 4 sites in Sabarkantha. Wells 13 and 16 are located near the Kundol and Harnav reservoirs, respectively,
where irrigation is primarily supported by surface water during the non-monsoon season. Well 14 lies
in an area where no agriculture is practiced during the rabi season, reducing year-round pumping. Well
15 is situated within a settlement zone with limited agricultural activity. Additionally, farmers often
refrained from growing crops during the non-monsoon season. As a result, groundwater extraction
730 occurs only for a limited duration, and its impact on groundwater level is likely minimal over the long
term. The consistently low CRPS values at these wells, together with the field evidence of limited
groundwater abstraction, suggests that CRPS provides a reliable basis for identifying climate-dominated
sites.

On land cover change, the historical land use patterns near selected wells provides additional context
735 for interpreting groundwater residual trend. For instance, an analysis of land use changes for well 32
shows a shift from agricultural land (pre-2010) to scrubland and eventually barren land by 2020 (Fig.
S2). This transition suggests that groundwater fluctuations in this region are influenced by both climate
and anthropogenic factors. The CRPS values for well 32 was above the adopted threshold of 0.80 over
four- and eight-year periods, indicating it to be not climate-dominated. Furthermore, the residuals have
740 a positive slope, suggesting a driver other than pumping. This consistency between the modeling results
and the complex land use transition around well 32 is encouraging, though we encourage others to
further examine this issue.

Despite these independent lines of validation, the analysis remains subject to uncertainty arising from
the use of gridded meteorological inputs for rainfall, temperature, and potential evapotranspiration.
745 Long-term meteorological observations were not available at most well locations, necessitating reliance
on India Meteorological Department (IMD) gridded datasets. While these products are derived from
station observations and are widely used in hydro-climatological studies across India, their spatial
resolution may not fully capture local-scale variability in rainfall and temperature. Uncertainty in PET
estimation represents an additional limitation, particularly given the use of the temperature-based
750 Hargreaves formulation under data-limited conditions. However, within the HydroSight framework,
PET affects groundwater heads only indirectly through recharge estimation, and recharge signals are
subsequently smoothed through convolution and groundwater storage processes. As a result, short-
term errors or excessive day-to-day variability in PET are substantially attenuated in the simulated
groundwater response. Importantly, if uncertainties in rainfall or PET led to unrealistic recharge
755 dynamics, this would lead to poor calibration or predictive performance, and such wells would not be
classified as climate-dominated, therefore a potential under-identification of climate-dominated wells,
rather than false attribution of climatic control. However, the fact that a substantial number of wells
exhibit both good calibration and sustained predictive skill over independent evaluation periods
indicates that the influence of meteorological input uncertainty on the main conclusions is modest.



760 We further compared our results with the independent government assessments carried out in the region.
The CGWB classifies groundwater extraction levels at an administrative scale ranging from “safe” to
“overexploited”. As discussed in Section 2.1, their approach appears to rely on estimates of crop type
and electricity usage but does not account for the impact of climate variability or evaluate their results
against observed groundwater levels. That said, Fig. S3 shows the spatial distribution of groundwater
765 extraction status for the year 2020 across North Gujarat. A large portion of the region is categorized as
“overexploited”, where annual extraction exceeds available recharge—with a greater concentration of
overexploited blocks in Banaskantha and Mehsana districts, followed by parts of Patan and
Sabarkantha. In contrast, Aravalli district is entirely classified as “safe”, and most blocks in Sabarkantha
district also fall within the safe or semi-critical categories, indicating relatively sustainable groundwater
770 use. Similarly, our analysis of climate and groundwater head suggests that regions such as the western
and central blocks of Banaskantha district and the northern blocks of Mehsana district are likely
impacted by groundwater pumping. This aligns with CGWB findings, which is encouraging. However,
our results provide significantly greater spatial nuance. While CGWB may categorize an entire block
as overexploited, our analysis reveals that some wells within those blocks respond primarily to climate
775 signals, not pumping. For instance, in the central part of the region—particularly along the Mehsana–
Patan border—our method identified wells influenced by climate variability, even though these areas
are classified as overexploited or saline by CGWB. This highlights the limitations of using regional
scale assessments not informed by groundwater level observations. In contrast, our approach is based
directly on groundwater hydrograph analysis and model-based prediction using observed head data,
780 providing a more evidence-based and dynamic understanding of groundwater change attribution. By
identifying local drivers of stress, our approach can inform more targeted interventions—such as
regulating extraction in pumping-dominated areas or enhancing recharge where climate influence is
dominant—ultimately supporting more adaptive and sustainable groundwater management.

5 Conclusion

785 This study demonstrates that identifying climate-dominated groundwater systems requires evaluation
beyond calibration-period hydrograph fit. Using the HydroSight time-series modelling framework
(Peterson and Western, 2014; Peterson and Fulton, 2019) across 92 wells across North Gujarat, we
found that many wells classified as climate-dominated during calibration did not maintain predictive
skill when evaluated against independent observations, indicating the influence of other non-climatic
790 factors. In contrast, across evaluation periods of 2, 4 and 8 years, 51%, 48% and 37% of wells,
respectively, maintained climate-dominated performance prediction. These wells showed spatial
coherence and were concentrated in the eastern part of the North Gujarat region, where low-intensity
agriculture is consistent with limited abstraction.

Beyond the regional case study, the findings provide a transferable framework for groundwater driver
795 attribution. By combining statistical time-series modelling with explicit predictive evaluation, the



approach captures spatial heterogeneity in groundwater responses that aggregated or administrative-scale assessments often overlook, enabling more targeted management responses. Wells exhibiting sustained climate-dominated behavior are more likely to benefit from recharge enhancement and watershed-scale interventions, whereas wells showing anthropogenic influence require demand-side
800 measures such as improved irrigation efficiency, crop diversification, or regulated abstraction.

Looking longer-term, metered groundwater pumping is likely to remain a limiting factor in understanding the drivers of groundwater change—because metering rarely extends over the duration of extractions—including in high-income countries. As a result, groundwater assessments will continue for many years to rely on indirect attribution frameworks based on groundwater level responses to
805 climate variability. The framework developed here therefore provides a broadly applicable basis for groundwater driver attribution where direct abstraction data are unavailable.

Overall, this study advances groundwater assessment by demonstrating that predictive evaluation, rather than calibration fit alone, is central to reliable driver attribution. The framework provides a practical and scalable basis for distinguishing climatic and anthropogenic influences on groundwater
810 levels and can be extended to a wide range of hydrogeological and climatic settings to support more informed groundwater management and policy decisions.

Code and Data availability

The time-series groundwater level data and location coordinates across India are available on the India Water Resources Information System (WRIS), created as a part of the National Hydrology Project of
815 the Ministry of Jal Shakti, The Department of Water Resources, River Development and Ganga Rejuvenation (DoWR, RD & GR), Government of India and is available at <https://indiawris.gov.in/wris/#/groundWater>. The climate data at the given groundwater well locations is extracted using bilinear interpolation in Rstudio from the gridded high-resolution Indian Meteorological Department (IMD) data, available at
820 https://cdsp.imdpune.gov.in/home_gridded_data.php. The groundwater hydrograph modelling software HydroSight version 1.41.1.5 (Peterson & Western, 2014; Peterson & Fulton, 2019) is used and actively maintained at <https://github.com/peterson-tim-j/HydroSight>.

Author Contribution

MG : Conceptualization, Data curation, Formal analysis, Investigation, Methodology, Validation,
825 Visualization, Writing – Original draft preparation, Writing- review and editing

TP: Conceptualization, Methodology, Supervision, Writing – review and editing

Competing Interest

The authors declare that they have no competing interest.



References

- 830 Census of India. (2011). *Primary census abstracts*. Registrar General of India, Ministry of Home Affairs, Government of India.
- CGWB (Central Ground Water Board). (2020). *Technical Report Series: Aquifer Mapping and Management of Groundwater Resources, Patan District, Gujarat*. West Central Region, Ahmedabad, Central Ground Water Board, Department of Water Resources, RD and GR, Ministry of Jal Shakti, Government of India.
- 835 CGWB (Central Ground Water Board). (2021). *Groundwater year book 2020-21, Gujarat State*. Regional office Data Centre, Central Groundwater Board, West Central Region- Ahmedabad, Department of Water Resources, River Development and Ganga Rejuvenation, Ministry of Jal Shakti, Government of India.
- 840 CGWB (Central Ground Water Board). (2022). *National compilation on dynamic groundwater resources of India, 2022*. Department of Water Resources, River Development and Ganga Rejuvenation, Ministry of Jal Shakti, Government of India.
- Collenteur, R. A., Haaf, E., Bakker, M., Liesch, T., Wunsch, A., Soonthornrangsang, J., ... & Meysami, R. (2024). Data-driven modelling of hydraulic-head time series: results and lessons learned from the 2022 Groundwater Time Series Modelling Challenge. *Hydrology and Earth System Sciences*, 28(23), 5193-5208.
- 845 Condon, L. E., Kollet, S., Bierkens, M. F., Fogg, G. E., Maxwell, R. M., Hill, M. C., ... & Abesser, C. (2021). Global groundwater modeling and monitoring: Opportunities and challenges. *Water Resources Research*, 57(12), e2020WR029500. <https://doi.org/10.1029/2020WR029500>.
- 850 de Graaf, I. E., van Beek, R. L., Gleeson, T., Moosdorf, N., Schmitz, O., Sutanudjaja, E. H., & Bierkens, M. F. (2017). A global-scale two-layer transient groundwater model: Development and application to groundwater depletion. *Advances in water Resources*, 102, 53-67. <https://doi.org/10.1016/j.advwatres.2017.01.011>
- Fabbri, P., Piccinini, L., Marcolongo, E., Pola, M., Conchetto, E., & Zangheri, P. (2016). Does a change of irrigation technique impact on groundwater resources? A case study in Northeastern Italy. *Environmental Science & Policy*, 63, 63-75. <https://doi.org/10.1016/j.envsci.2016.05.009>
- 855 Fan, X., Peterson, T. J., Henley, B. J., & Arora, M. (2023). Groundwater sensitivity to climate variations across Australia. *Water Resources Research*, 59(11), e2023WR035036. <https://doi.org/10.1029/2023WR035036>
- 860 Famiglietti, J. S., & Rodell, M. (2013). Water in the balance. *Science*, 340(6138), 1300-1301. <https://doi.org/10.1126/science.1236460>



- Fowler, K., Knoben, W., Peel, M., Peterson, T., Ryu, D., Saft, M., Seo, K.W., & Western, A. (2020). Many commonly used rainfall-runoff models lack long, slow dynamics: Implications for runoff projections. *Water Resources Research*, 56(5), e2019WR025286.
865 <https://doi.org/10.1029/2019WR025286>
- Frommen, T., Groeschke, M., Nölscher, M., Koeniger, P., & Schneider, M. (2021). Anthropogenic and geogenic influences on peri-urban aquifers in semi-arid regions: insights from a case study in northeast Jaipur, Rajasthan, India. *Hydrogeology Journal*, 29(3), 1261-1278.
<https://doi.org/10.1007/s10040-021-02301-7>
- 870 Gneiting, T., & Raftery, A. E. (2007). Strictly proper scoring rules, prediction, and estimation. *Journal of the American statistical Association*, 102(477), 359-378.
<https://doi.org/10.1198/016214506000001437>
- Greve, P., Gudmundsson, L., Orłowsky, B., & Seneviratne, S. I. (2015). Introducing a probabilistic Budyko framework. *Geophysical Research Letters*, 42(7), 2261-2269.
875 <https://doi.org/10.1002/2015GL063449>
- GSI (Geological Survey of India). (1970). *Geological and mineral map of Gujarat, First Edition -1970*. Government of India.
- Han, D., Currell, M. J., Cao, G., & Hall, B. (2017). Alterations to groundwater recharge due to anthropogenic landscape change. *Journal of hydrology*, 554, 545-557.
880 <https://doi.org/10.1016/j.jhydrol.2017.09.018>
- Hansen, N. (2006). The CMA Evolution Strategy: A Comparing Review. In: Lozano, J.A., Larrañaga, P., Inza, I., Bengoetxea, E. (eds) *Towards a New Evolutionary Computation. Studies in Fuzziness and Soft Computing*, vol 192. Springer, Berlin, Heidelberg. https://doi.org/10.1007/3-540-32494-1_4
- 885 Hargreaves, G. H., & Samani, Z. A. (1985). Reference crop evapotranspiration from temperature. *Applied engineering in agriculture*, 1(2), 96-99. <https://doi.org/10.13031/2013.26773>
- Healy, R. W., & Cook, P. G. (2002). Using groundwater levels to estimate recharge. *Hydrogeology journal*, 10, 91-109. <https://doi.org/10.1007/s10040-001-0178-0>
- Hijmans, R. J., Van Etten, J., Cheng, J., Mattiuzzi, M., Sumner, M., Greenberg, J. A., ... & Hijmans, M. R. J. (2015). Package 'raster'. *R package*, 734, 473.
- 890 Hoogesteger, J. (2022). Regulating agricultural groundwater use in arid and semi-arid regions of the Global South: Challenges and socio-environmental impacts. *Current Opinion in Environmental Science & Health*, 27, 100341. <https://doi.org/10.1016/j.coesh.2022.100341>
- Jordan, A., Krüger, F., & Lerch, S. (2017). Evaluating probabilistic forecasts with scoringRules. *arXiv preprint arXiv:1709.04743*. <https://doi.org/10.18637/jss.v090.i12>
895



- Krzysztofowicz, R. (2001). The case for probabilistic forecasting in hydrology. *Journal of hydrology*, 249(1-4), 2-9. [https://doi.org/10.1016/S0022-1694\(01\)00420-6](https://doi.org/10.1016/S0022-1694(01)00420-6)
- Ladson, A. R. (2008) *Hydrology: An Australian Introduction*. Oxford University Press.
- McDermid, S., Nocco, M., Lawston-Parker, P., Keune, J., Pokhrel, Y., Jain, M., ... & Yokohata, T. (2023). Irrigation in the Earth system. *Nature Reviews Earth & Environment*, 4(7), 435-453. <https://doi.org/10.1038/s43017-023-00438-5>
- Mistry, P., & Suryanarayana, T. M. V. (2021). Study of groundwater recharge estimation using empirical equations in North Gujarat, India. India (March 17, 2021). <https://dx.doi.org/10.2139/ssrn.3806570>
- Moriasi, D. N., Arnold, J. G., Van Liew, M. W., Bingner, R. L., Harmel, R. D., & Veith, T. L. (2007). Model evaluation guidelines for systematic quantification of accuracy in watershed simulations. *Transactions of the ASABE*, 50(3), 885-900. <https://dx.doi.org/10.13031/2013.23153>
- MoWR, RD & GR (Ministry of Water Resources, River Development & Ganga Rejuvenation). (2017). *Report of the Groundwater Resource Estimation Committee (GEC 2015) : Methodology*. Ministry of Water Resources, River Development & Ganga Rejuvenation. New Delhi.
- Nash, J. E., & Sutcliffe, J. V. (1970). River flow forecasting through conceptual models part I—A discussion of principles. *Journal of hydrology*, 10(3), 282-290. [https://doi.org/10.1016/0022-1694\(70\)90255-6](https://doi.org/10.1016/0022-1694(70)90255-6)
- Ojha, R., Ramadas, M., & Govindaraju, R. S. (2015). Current and future challenges in groundwater. I: Modeling and management of resources. *Journal of Hydrologic Engineering*, 20(1), A4014007. [https://doi.org/10.1061/\(ASCE\)HE.1943-5584.0000928](https://doi.org/10.1061/(ASCE)HE.1943-5584.0000928).
- Oreskes, N., Shrader-Frechette, K., & Belitz, K. (1994). Verification, validation, and confirmation of numerical models in the Earth sciences. *Science*, 263(5147), 641–646. <https://doi.org/10.1126/science.263.5147.641>.
- Owuor, S. O., Butterbach-Bahl, K., Guzha, A. C., Rufino, M. C., Pelster, D. E., Díaz-Pinés, E., & Breuer, L. (2016). Groundwater recharge rates and surface runoff response to land use and land cover changes in semi-arid environments. *Ecological Processes*, 5, 1-21. <https://doi.org/10.1186/s13717-016-0060-6>
- Pebesma, E., Bivand, R., Pebesma, M. E., RColorBrewer, S., & Collate, A. A. A. (2012). Package ‘sp’. *The Comprehensive R Archive Network*, 9.
- Peel, M. C., Finlayson, B. L., & McMahon, T. A. (2007). Updated world map of the Köppen-Geiger climate classification. *Hydrology and earth system sciences*, 11(5), 1633-1644. <https://doi.org/10.5194/hess-11-1633-2007>
- Peterson, T. J., & Western, A. W. (2014). Non-linear time-series modeling of unconfined groundwater head. *Water Resources Research*, 50(10), 8330-8355. <https://doi.org/10.1002/2013WR014800>



- 930 Peterson, T. J., Western, A. W., & Cheng, X. (2018). The good, the bad and the outliers: automated detection of errors and outliers from groundwater hydrographs. *Hydrogeology Journal*, 26(2), 371-380. <https://doi.org/10.1007/s10040-017-1660-7>
- Peterson, T. J., & Fulton, S. (2019). Joint estimation of gross recharge, groundwater usage, and hydraulic properties within HydroSight. *Groundwater*, 57(6), 860-876.
935 <https://doi.org/10.1111/gwat.12946>
- Pool, S., Francés, F., Garcia-Prats, A., Puertes, C., Pulido-Velazquez, M., Sanchis-Ibor, C., ... & Jiménez-Martínez, J. (2022). Impact of a transformation from flood to drip irrigation on groundwater recharge and nitrogen leaching under variable climatic conditions. *Science of the Total Environment*, 825, 153805. <https://doi.org/10.1016/j.scitotenv.2022.153805>
- 940 Porhemmat, J., Nakhaei, M., Dadgar, M. A., & Biswas, A. (2018). Investigating the effects of irrigation methods on potential groundwater recharge: A case study of semi-arid regions in Iran. *Journal of Hydrology*, 565, 455-466. <https://doi.org/10.1016/j.jhydrol.2018.08.036>
- Scanlon, B. R., Reedy, R. C., Stonestrom, D. A., Prudic, D. E., & Dennehy, K. F. (2005). Impact of land use and land cover change on groundwater recharge and quality in the southwestern US. *Global Change Biology*, 11(10), 1577-1593. <https://doi.org/10.1111/j.1365-2486.2005.01026>
945
- Scanlon, B. R., Faunt, C. C., Longuevergne, L., Reedy, R. C., Alley, W. M., McGuire, V. L., & McMahon, P. B. (2012). Groundwater depletion and sustainability of irrigation in the US High Plains and Central Valley. *Proceedings of the national academy of sciences*, 109(24), 9320-9325. <https://doi.org/10.1073/pnas.1200311109>
- 950 Shapoori, V., Peterson, T. J., Western, A. W., & Costelloe, J. F. (2015a). Top-down groundwater hydrograph time-series modeling for climate-pumping decomposition. *Hydrogeology Journal*, 23(4), 819-836. <https://doi.org/10.1007/s10040-014-1223-0>
- Shapoori, V., Peterson, T. J., Western, A. W., & Costelloe, J. F. (2015b). Decomposing groundwater head variations into meteorological and pumping components: a synthetic study. *Hydrogeology Journal*, 23(7), 1431-1448. <https://doi.org/10.1007/s10040-015-1269-7>
955
- Sharda, V. N., Kurothe, R. S., Sena, D. R., Pande, V. C., & Tiwari, S. P. (2006). Estimation of groundwater recharge from water storage structures in a semi-arid climate of India. *Journal of Hydrology*, 329(1-2), 224-243. <https://doi.org/10.1016/j.jhydrol.2006.02.015>
- 960 Siddik, M. S., Tulip, S. S., Rahman, A., Islam, M. N., Haghghi, A. T., & Mustafa, S. M. T. (2022). The impact of land use and land cover change on groundwater recharge in northwestern Bangladesh. *Journal of Environmental Management*, 315, 115130. <https://doi.org/10.1016/j.jenvman.2022.115130>



- 965 Siebert, S., Burke, J., Faures, J. M., Frenken, K., Hoogeveen, J., Döll, P., & Portmann, F. T. (2010).
Groundwater use for irrigation—a global inventory. *Hydrology and earth system sciences*, 14(10),
1863-1880. <https://doi.org/10.5194/hess-14-1863-2010>
- Sukhija, B. S., & Shah, C. R. (1976). Conformity of groundwater recharge rate by tritium method and
mathematical modelling. *Journal of Hydrology*, 30(1-2), 167-178. [https://doi.org/10.1016/0022-1694\(76\)90096-2](https://doi.org/10.1016/0022-1694(76)90096-2)
- 970 Sukhija, B. S., Nagabhushanam, P., & Reddy, D. V. (1996). Groundwater recharge in semi-arid regions
of India: an overview of results obtained using tracers. *Hydrogeology Journal*, 4, 50-71.
<https://doi.org/10.1007/s100400050089>
- Tam, V. T., & Nga, T. T. V. (2018). Assessment of urbanization impact on groundwater resources in
Hanoi, Vietnam. *Journal of environmental management*, 227, 107-116.
<https://doi.org/10.1016/j.jenvman.2018.08.087>
- 975 Taylor, R. G., Scanlon, B., Doll, P., Rodell, M., van Beek, R., Wada, Y., et al. (2013). Ground water
and climate change. *Nature Climate Change*, 3(4), 322–329. <https://doi.org/10.1038/nclimate1744>
- Van Der Spek, J. E., & Bakker, M. (2017). The influence of the length of the calibration period and
observation frequency on predictive uncertainty in time series modeling of groundwater dynamics.
Water Resources Research, 53(3), 2294-2311. <https://doi.org/10.1002/2016WR019704>
- 980 Wunsch, A., Liesch, T., & Broda, S. (2022). Deep learning shows declining groundwater levels in
Germany until 2100 due to climate change. *Nature communications*, 13(1), 1221.
<https://doi.org/10.1038/s41467-022-28770-2>